Depth-Based Method for Target Detection in Noisy Environments

James Paul Browning and Hugh D. Griffiths
Department of Electronic and Electrical Engineering
University College London
London, UK
Email: ud2006alumni@me.com
Email: h.griffiths@ucl.ac.uk

Jeremy Entner and Pinyuen Chen
Department of Mathematics
Syracuse University
Syracuse, NY USA
Email: jfe2950@jeremyentner.com
Email: pinchen@syr.edu

***Abstract*—In this paper we introduce a novel non-parametric depth-based method for the target detection problem in noisy environments under nominal signal-to-noise ratios. Specifically, a distributed sensor network comprised of multiple transceivers is considered. Each sensor is able to transmit and receive a single tone; which is passed to a *super sensor* where the data is formed into a multistatic response matrix via a pre-detection fusion algorithm. An algorithm is introduced for the determination of the presence of a target in the background medium. The detection performance versus signal-to-noise ratio is developed for a given false alarm rate and compared to a typical monostatic sensor. The depth-based method is shown to improve upon the performance of a single sensor by a considerable margin.**

I. Introduction

One challenge in formulating predicted detection performance for a multi-sensor system, especially one utilizing waveform diversity, is that the traditional assumptions of Gaussianity are no longer valid. British mathematicians were able to show in the 1940's with one of the first operational radar continuous wave systems that measurements followed normal distributions; Rayleigh in the case of a magnitude detector. However, many different waveforms have been developed since the days of early radar systems, and not all of these waveforms have been shown to obey the Gaussian distribution when used for measurements-i.e. mathematically shown that the measurements obey a Gaussian distribution; when coupled with the desire to make use of multiple sensors for measurements-in which not every sensor may be transmitting the same waveform-there is a strong desire to look towards nonparametric methods for common sensor processing tasks-such as object detection.

In this paper we present a non-parametric depth-based method for the detection of an object in a background medium comprised of Gaussian noise; there is no need to limit ourselves to Gaussian noise, however for this initial introductory paper, Gaussian noise was chosen so that the detection performance can be readily compared to that of a monostatic radar sensor; which has been well documented, see [5], [7], [8] for examples. Specifically, a distributed sensor network comprised of multiple transceivers is considered. Each sensor is able to transmit and receive a single tone; which is passed to a *super sensor* where the data is formed into a multistatic response matrix via a pre-detection fusion algorithm. An algorithm is introduced for the determination of the presence of a bounded rank perturbation of the resultant multistatic response matrix. The detection performance versus signal-to-noise ratio is developed and compared to that of a typical monostatic sensor.

II. Sensor Networks

One major challenge for distributed sensing networks is the issue of data fusion. Put simply, what is the best method of taking all of the data generated by the network of sensors, and assembling the data deluge into a meaningful quantity that is able to be processed? One method would be to have each sensor transmit, receive and process data from the sensor network-in essence, each sensor is an active agent in the network, but processes data independently of its neighbors. An advantage to this system would be the redundancy built into the network, and the ability to parallelize tasks, and process the data more quickly. One disadvantage, would be the extreme cost of outfitting each sensor with its own transmitter, receiver, and processor.

Another sensor fusion concept could be that of a netted radar. In this system design, several radar are linked together to improve the coverage or accuracy of the radar net. This improvement comes from the union of individual coverage areas [12]. We could simplify the architecture of the radar net by using range-only data, which would result in a *multilateration radar* system.

If we assume the distributed network of sensors is comprised of two sensors, a transmitter and a receiver, then we have a bistatic radar system; where the transmitter and receiver are separated by a considerable distance in order to achieve some benefit: technical, operational, or cost [12]. Further, if the sensor network was comprised of a number of bistatic systems with multiple transmitters and receivers, then we have a multistatic radar network.

In our case, we assume each sensor has a transmitter and receiver. Additionally, the sensors are relatively simple, and only transmit and receiver a single tone (which can change from pulse-to-pulse, or cpi-to-cpi if required). Each

2013 IEEE Radar Conference (RadarCon13)

sensor collects the received signal from each transmitter and sends this data to a super-sensor. This super-sensor takes the accumulated big data and formats and/or stores the data for real-time or near real-time processing. The super-sensor has only a communications system that is capable of transmitting and receiving information from each sensor in the network, but does not participate in the sensing activities of the network. In this manner, the sensor network is actually a layered system of systems, comprising a separate processing platform from the relatively simple and low-cost sensing systems.

III. Response Matrix Formulation

Having defined the sensor network utilized for this scenario, we now turn our attention to the pre-detection fusion process that will result in a *multistatic response matrix*, which is processed by our super-sensor. To limit the number of variables feeding into our simulation, we constrain the operations of the sensor network to that of two-dimensions. The sensor network is comprised of a total of m transmitters and n receivers, located at positions $\mathbf{y}_n = (n = 1, 2, \ldots, N)$ and $\mathbf{z}_m \, (m = 1, 2, \ldots, M)$, respectively.

Each of the transmitters sends out a wave, which impinges upon an object; this object, in turn, re-radiates a portion of the incident wave energy isotropically. The field received by the n^{th} receiving element $\mathbf{y}_n$ when the wave is emitted from the m^{th} transmitter element $\mathbf{z}_m$ is $\hat{u}\left(\mathbf{y}_n, \mathbf{z}_m\right)$. If we remove the incident field then we obtain the $(n, m)^{th}$ entry of the corresponding multistatic response matrix [9]

$$A_{nm} = \hat{u}\left(\mathbf{y}_n, \mathbf{z}_m\right) - \hat{G}\left(\omega, \mathbf{y}_n, \mathbf{z}_m\right) \tag{1}$$

The incident field is the homogeneous Green's function given by $G\left(\omega, \mathbf{x}, \mathbf{y}\right)$, which for two-dimensions is of the form

$$\hat{G}\left(\omega, \mathbf{x}, \mathbf{y}\right) = \frac{i}{4} H_0^{(1)}\left(\frac{\omega}{c_0} \mid \mathbf{y} - \mathbf{x} \mid\right) \tag{2}$$

with $H_0^{(1)}$ representing a Hankel function of the first-kind, zeroth-order, and the vector $\mathbf{x}$ is the location of the object to be detected.

In the Born approximation, the volume for $\Omega_j, j = 1, \ldots, r$ goes to zero, and the measured field is approximated by the expression

$$\hat{u}\left(\mathbf{y}_n, \mathbf{z}_m\right) = \hat{G}\left(\omega, \mathbf{y}_n, \mathbf{z}_m\right) + \sum_{j=1}^{r} \rho_j \hat{G}\left(\omega, \mathbf{y}_n, \mathbf{x}_j\right) \hat{G}\left(\omega, \mathbf{x}_j, \mathbf{z}_m\right) \tag{3}$$

for all transmitter and receiver locations n and m. The coefficient ρ_j is the reflection coefficient and is defined by the quantity

$$\rho_j = \frac{\omega^2}{c_0^2} \eta_j l_j^2 \tag{4}$$

We determine the singular value from the expression [9]

$$\sigma_j := \rho_j \left(\sum_{n=1}^{N} \mid \hat{G}\left(\omega, \mathbf{x}_j, \mathbf{y}_n\right) \mid^2\right)^{\frac{1}{2}} \left(\sum_{m=1}^{M} \mid \hat{G}\left(\omega, \mathbf{x}_j, \mathbf{z}_m\right) \mid^2\right)^{\frac{1}{2}} \tag{5}$$

where $\hat{G}\left(\omega, \mathbf{x}_j, \mathbf{y}_n\right)$ is the general form of the receiver array Green's functions and $\hat{G}\left(\omega, \mathbf{x}_j, \mathbf{z}_m\right)$ is the general form of the transmitter array Green's functions. To formulate the multistatic response matrix, it is also necessary to calculate the normalized vector of Green's functions for the transmitter and receiver array. The normalized vector of Green's functions for the receiver array to the reflector point specified by $\mathbf{x}$ is given by

$$\mathbf{u}\left(\mathbf{x}\right) := \frac{1}{\left(\sum_{l=1}^{N} \mid \hat{G}\left(\omega, \mathbf{x}, \mathbf{y}_l\right) \mid^2\right)^{\frac{1}{2}}} \left(\hat{G}\left(\omega, \mathbf{x}, \mathbf{y}_n\right)\right)_{n=1,\ldots,N} \tag{6}$$

The normalized vector of Green's functions for the transmitter array from the reflector point specified by $\mathbf{x}$ is given by

$$\mathbf{v}\left(\mathbf{x}\right) := \frac{1}{\left(\sum_{l=1}^{M} \mid \hat{G}\left(\omega, \mathbf{x}, \mathbf{z}_l\right) \mid^2\right)^{\frac{1}{2}}} \left(\overline{\hat{G}\left(\omega, \mathbf{x}, \mathbf{z}_n\right)}\right)_{m=1,\ldots,M} \tag{7}$$

Having solved for the target singular value and the normalized vector of Green's functions for the transmitter and receiver array, the response matrix is determined from the following [10]

$$\mathbf{A} = \sum_{j=1}^{r} \sigma_j \mathbf{u}\left(\mathbf{x}_j\right) \mathbf{v}\left(\mathbf{x}_j\right)^* \tag{8}$$

We note that (8) is of bounded rank, r, and positive semidefinite.

A. Measurement Noise

We can assume the measurements will contain additive noise, represented by an $N \times M$ matrix, $\mathbf{W}$, which is considered a matrix of independent and identically distributed complex entries with arbitrary statistics. This noise is an additive mixture of environmental and receiver system noise. The resultant measured response matrix is then

$$\mathbf{B} = \mathbf{A} + \frac{1}{\sqrt{M}} \mathbf{W} \tag{9}$$

(9) is valid for the non-trivial asymptotic regimes in the limit $M \to \infty$; so the scaling factor $\frac{1}{\sqrt{M}}$ is appropriate [10].

IV. Introduction to Depth-Based Methods

A. Introduction to Half-Space Depth and Associated Properties

Give k multivariate populations $\pi_i = \pi\left(P_i\right)$ on $\mathbb{R}^d$, $d > 1$, with absolutely continuous distributions P_i, defined on random variables X_i for $i = 1, \ldots, k$ we propose a procedure for selecting the "most dispersed" member from a group k populations. We define our measure of dispersion in terms of the depth-based scale curve introduced by Liu, et al. in [3]. The scale curves if $\mathcal{P}$ is the collection of probability distributions, we may consider a depth function to be any bounded, nonnegative mapping $D\left(\cdot;\cdot\right) : \mathbb{R}^d \times \mathcal{P} \to \mathbb{R}$ that provides a probability based center-outward ordering of points

in $\mathbb{R}^d$. For the center-outward ranking, we will make use of Tukey's Half-Space Depth [1], [2]

$$D(x;P) = \inf\{P(H)\,|x \in H, H\text{is a closed half-space}\} \tag{10}$$

where $x \in \mathbb{R}$. This half-space depth has four primary properties that provide insight into the power and utility of depth-based measures, these properties were proposed in [6]

1) $D(Ax+b;\ P_{Ax+b}) = D(x;\ P_X)$ for any random vector $X \in \mathbb{R}^d$, and $d \times x$ nonsingular matrix A, and any $d \times 1$vector b.
2) For any $P \in P$ with center Θ, then $D(\Theta;\ P) = \sup_x D(x;\ P)$.
3) If Θ is the deepest point for any $P \in \mathcal{P}$, then $D(x;\ P) \leq D(\Theta + \alpha(x-\Theta);\ P)$ for $\alpha \in [0,1]$.
4) $D(x;\ P) \to 0$ as $\|x\| \to \infty$ for any $P \in \mathcal{P}$.

B. Depth-Regions and Measures of Dispersion

Application of property (1) allows for the definition of α-*trimmed depth-regions* of P,

$$D^\alpha(P) = \left\{x \in \mathbb{R}^d | D(x;P) \geq \alpha\right\} \tag{11}$$

If we solve for the volume of a particular α-*trimmed depth-region*, we have *de facto* solved for the dispersion of that same region. In order to compare the dispersion of one population with that of a second population, we introduce the concept of a *scale curve*. The scale curve is the volume, or dispersion, and is defined as

$$V^p = \inf\{\text{Volume}(D^\alpha(P))\,|P(D^\alpha(P)) \geq p,\ 0 < \alpha < \alpha^*\} \tag{12}$$

with $p \in (0,1)$ and where $\alpha^* = \sup_{x \in \mathbb{R}^d} D(x;\ P)$.

Definition 1. *For $p \in (0,1)$, we say that π_i is more dispersed, or more concentrated, than π_j (at level p), if $V_i^p \geq V_j^p$ is the volume from population π_i.*

If P is absolutely continuous, according to [6], the collections of $D^\alpha(P)$ based on the half-space depth are affine equivariant, nested, connected, and compact for $p \in (0,1)$.

C. Empirical Distribution

For any given set of data, let $X_{i,1}, X_{i,2}, \ldots, X_{i,n}$ be a random sample from P_i for a random variable X_i, and B be a Borel set, the empirical distribution is defined as

$$P_{i,n}(B) = \frac{1}{n}\sum_{j=1}^{n} I_B(X_{i,j}) \tag{13}$$

with $I_B(x)$ being an indicator function for B.

D. Depth-Based Detection

In order to formulate the hypothesis test, we need to first define the two populations that will be compared. The first population considered is that of a general class of arbitrary distribution, representative of the background medium-i.e. noise. The second population is a measured multistatic response matrix consisting of a bounded rank signal perturbation with additive noise; in which the noise is scaled to simulate a set of signal-to-noise sample values. From these two populations, we define a new depth-based detection statistic, but first let us revisit the binary hypothesis test utilized for our example.

$$\begin{aligned} H_0 &:= n(t) \\ H_1 &:= s(t) + n(t) \end{aligned} \tag{14}$$

Typically, we measure a component of the received signal and compare this value to a pre-determined, or adaptive, threshold that allows us to transform equation (14) into

$$\delta_{\text{threshold}} \underset{>H_1}{\overset{\leq H_0}{}} \tag{15}$$

with the null hypothesis indicating the absence of a signal. The depth-based detection method is also based on a threshold statistic, determined from a ratio of two dispersion values,

$$\frac{\hat{V}_{[i]}}{\hat{V}_{[\text{threshold}]}} = \delta \tag{16}$$

in which $\hat{V}_{[i]}$ and $\hat{V}_{[\text{threshold}]}$ are the differential dispersion values for the populations of the measured multistatic response matrix and noise matrix with arbitrary distribution, respectively. Differential dispersion values are derived from the difference of two dispersion values, as shown below

$$\hat{V}_{[\text{threshold}]} = \hat{V}^\beta_{\text{threshold}} - \hat{V}^p_{\text{threshold}} \tag{17}$$

The differential dispersion is the difference between the volume defined by the contour β, and that of the volume of a second contour p. Typically, we define $\beta \simeq 1$, to ensure we incorporate all of the population values in our depth functional; the second dispersion is found from a smaller contour defined by $p \in (0,1)$. In this instance, we have defined $p = [0.5, 0.75, 0.9]$. The difference between these two contours defines the volume of an annular region, $\hat{V}_{[\text{threshold}]}$; with an increase in the annular region being attributed to the presence of a signal. We compare the differential dispersion of the assume noise threshold, with that of the measured data. In this manner, the second differential dispersion value in the threshold statistic is given as

$$\hat{V}_{[i]} = \hat{V}_i^\beta - \hat{V}_i^p \tag{18}$$

The depth-based detection binary hypothesis test is now akin to

$$\delta \underset{>H_1}{\overset{\leq H_0}{}} \delta_{\text{threshold}} \tag{19}$$

where the $\delta_{\text{threshold}}$ is determined for a given class of measurement noise. For the purpose of this paper, the threshold is found empirically through a Monte Carlo simulation; a large number of noise realizations were created, for two population groups of white Gaussian noise comprised of 124 singular values, to determine the empirical volume of the annular region bounded by the contour D^p and D^β; this Monte Carlo simulation was repeated several times to ensure a consistent estimator for the empirical mean μ and standard deviation σ.

For each instance, the empirical volume is calculated for the annulus by subtracting the volume of the $p = [0.5, 0.75, 0.9]$ contours from the $p_{max} = 1$ contour. The mean and variance for the volume of the annular region is listed in table I

$Vol_{p^{th}}$ Annulus	$\overline{\mu}$	$\overline{\sigma}$	$V_{\text{empirical}}$
90%	0.0016	$3.2e^{-4}$	$\overline{\mu} + k\overline{\sigma}$
75%	0.0011	$3.2e^{-4}$	$\overline{\mu} + k\overline{\sigma}$
50%	$4.3e^{-4}$	$2.3e^{-4}$	$\overline{\mu} + k\overline{\sigma}$

TABLE I: Empirical Thresholds

From Chebyshev's Inequatlity, we know that for any distribution in which the standard deviation is defined, the variables that fall within a certain number of standard deviations from the defined mean, $k\sigma$, is *at least as much as* [4]

Minimum Population from the Mean	Number of Standard Deviations (k)
50%	$\sqrt{2}$
75%	2
89%	3
94%	4
96%	5
97%	6
$1 - \frac{1}{k^2}\%$	k

TABLE II: Empirical Threshold Table

From II, we see that for an empirical false alarm rate of 6%, we would require the $\hat{V}_{\text{threshold}}$, $\mu + k\sigma$, to be equivalent to $\mu + 4\sigma$; likewise for an empirical false alarm rate of 4% and 3%, we require the $\hat{V}_{\text{threshold}}$ to be $\mu + 5\sigma$ and $\mu + 6\sigma$, respectively. Further, the dispersion resulting from the addition of a signal in the measured noise is manifest from the outlying nature of the signal singular values, when compared to the body of the measured noise plus *a priori* noise distribution data depth functional [11]; which is true for nominal signal-to-noise ratios (SNR). This is due to the fact that the singular values associated with the signal exhibit a level of eigenvalue repulsion, allowing them to be separate from the body of the data depth functional, see figure 1; which is further manifest from an application of Newton's Third Law to the eigenvalues of the singular value decomposition of the multistatic response matrix. As the SNR decreases, this 'eigenvalue' repulsive force becomes weaker and the signal singular values become distributed on the outer contour of the data depth functional. From this vantage point, we are not seeking the point of deepest depth for signal detection, but the values for which the singular values are most outlying, and result in an increase in volume for a given annular contour bounded by $p^{th} \in (p, 1)$. Since we have defined the metric as the ratio of scale curves, and the false alarm rate is controlled by the empirical $\hat{V}_{\text{threshold}}$, in this manner the threshold is actually equivalent to unity, $\delta_{\text{threshold}} = 1$. The Chebyshev Inequality represents a more severe constraint on the detection statistic, and should be more robust, though may result in lower P_D versus SNR for a given P_{FA}.

Having determined the empirical threshold statistic for the hypothesis testing, the remainder of this paper is dedicated to a demonstration of the depth-based detection algorithm for a three objects corrupted by measurement noise.

V. Example

A. Problem Formulation

In this example, there three isotropic reflectors that are within the scene under illumination by the distributed sensing network. Since the Born approximation was utilized in order to develop the multistatic response matrix, the reflectivity of the target is fixed, with an associated volume of zero. The surrounding background medium is assumed to be that of free-space, with the manifestation of noise resulting from the receiver thermal noise and receiver system components. We further approximate the form of the noise to be white Gaussian noise, $\mathcal{N}(0, \sigma)$, with the variance fixed at a value of unity. The signal-to-noise ratio is varied from $-3dB$ to $10dB$ in order to capture a broad range of conditions resulting from the sensor network pre-detection fusion process. The resulting signal subspace rank is then three, with all other rank components being associated with the random noise process. As the noise is increased, the eigenvalue repulsion between the noise and signal begins to weakens; this weakening results in missed detections and the potential for false alarms.

Again, It is worth repeating that there is no set constraint on the underlying statistics for either the signal or the noise; white Gaussian noise was chosen so that the results of this novel depth-based detection method could be better compared against well known monostatic receiver operating characteristics.

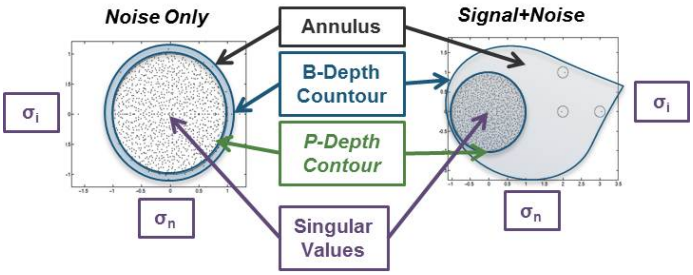

Fig. 1: Data Depth Functional Annular Volume Comparison for Noise Only versus Signal+Noise

B. Depth-Based Detector Performance: Nonparametric Case

In order to develop an adequate probability of detection curve, a Monte Carlo simulation was performed at each signal-to-noise ratio (SNR) sample . The number of Monte Carlo runs per SNR increment was large enough to ensure a representative sample point was captured that would be free from spurious statistical anomalies arising from the random noise process. A detection was recorded if, and only if, the annular volume increased sufficiently to exceed the detection threshold. For each $p^{th} = 0.5$ contour, the probability of detection was recorded for false alarm rates of 6% through 10^{-4}.

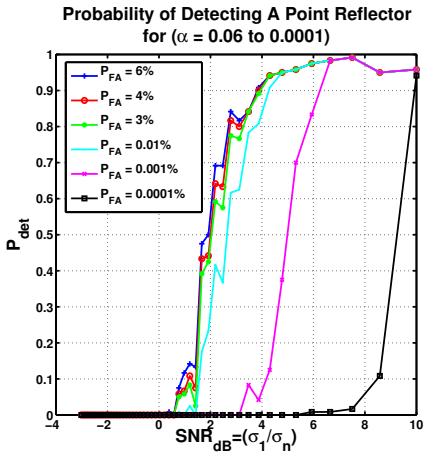

Fig. 2: P_D versus SNR for Depth-Based Detection Statistic

For comparison, if we assume a standard form of a radar detector, as found in [7], a performance comparison is possible for a single-pulse detector (no integration within the receiver for noise corruption described by a normal Gaussian distribution. The form of the detector is shown below

$$P_D = \frac{1}{2} - \Phi\left(x - \sqrt{2 \times SNR}\right) \tag{20}$$

where x is the detection threshold (such as 3 times the noise power) and Φ is the error function. The performance of the depth-based detector does indeed outperform the classical single-pulse detector, as shown in table III; for which the values of $P_D = 0.8$ are compared against the same P_{FA}.

P_{FA}	x	Required SNR for Classical Detector	Required SNR for Depth-Based Detector	Improvement Factor of Depth-Based Detector
6%	1.88	3.2 dB	2.8 dB	+0.4 dB
4%	2.05	4.2 dB	2.8 dB	+1.4 dB
3%	2.17	4.5 dB	3.2 dB	+1.3 dB
10^{-2}	2.33	5.1 dB	3.8 dB	+2.3 dB
10^{-3}	3.08	7.7 dB	5.8 dB	+1.9 dB
10^{-4}	3.62	10.0 dB	9.8 dB	+0.2 dB

TABLE III: Probability of Detection Comparison with Chebyshev Inequality

C. Knowledge-Aided Depth-Based Detector

However, the Chebyshev Inequality is a more restrictive detection criterion; which was chosen to ensure the depth-based detection algorithm is general for any given class of distribution-both known and unknown. We would expect the P_D would be less than that of equation (20), in which the function is derived on a normal Gaussian noise process assumption. In our example, the corruptive noise distribution is also assumed to be normal Gaussian; so, if we choose to re-run the same simulation by assuming our depth-function has complete *a priori* knowledge of the corruptive noise distribution, then the following false-alarm rates are more appropriate and are found from the error function, see table IV. We note, that owing to the conservative nature of the Chebyshev Inequality, the equivalent false-alarm rate-assuming Gaussian noise-for values greater than $P_{FA} > 10^{-2}$ are significantly better than those shown in table IV, but are purposefully kept to $\left(P_{FA} = 10^{-9}\right)$ and $(x = 6.23)$ for more relative comparisons of performance.

Chebyshev's Inequality, P_{FA}	$k\sigma$	x	Equivalent P_{FA} for Gaussian Noise
6%	4σ	3.62	10^{-4}
4%	5σ	4.75	10^{-6}
3%	6σ	5.61	10^{-8}
10^{-2}	10σ	$x \gg 6.23$	$P_{FA} \gg 10^{-9}$
10^{-3}	32σ	$x \gg 6.23$	$P_{FA} \gg 10^{-9}$
10^{-4}	100σ	$x \gg 6.23$	$P_{FA} \gg 10^{-9}$

TABLE IV: Probability of False Alarm for Knowledge-Aided Depth-Based Detector versus Classical Detector

For reliable detection performance, the probability of detection was set to $P_D = 0.8$. The Knowledge-Aided Depth-Based (KA-DB) detector in comparison with the classical single-pulse detector of equation (20) is given in table V; which does show significantly better performance; especially when the false alarm rate is low-ie $P_{FA} \leq 10^{-4}$.

$k\sigma$	Required SNR for Classical Detector	Required SNR for Depth-Based Detector	Improvement Factor of Depth-Based Detector
3σ	10.0 dB	2.8 dB	+7.2 dB
4σ	15.6 dB	2.8 dB	+12.8 dB
6σ	20.8 dB	3.2 dB	+17.6 dB
10σ	SNR$\gg$25 dB	3.8 dB	SNR$\gg$+21.2 dB
32σ	SNR$\gg$25 dB	5.8 dB	SNR$\gg$+19.2 dB
100σ	SNR$\gg$25 dB	9.8 dB	SNR$\gg$+15.2 dB

TABLE V: Probability of Detection Comparison for Knowledge-Aided Depth-Based Detector versus Classical Detector

D. Depth-Based and Knowledge-Aided Depth-Based Detector Performance versus Envelop Detector

More realistically, a radar will utilize the envelope of the received signal to perform the binary hypothesis test. If we assume a general form of the envelop detector [7]

$$SNR = A + 0.12AB + 1.7B \tag{21}$$

with $A = ln\frac{0.62}{P_{FA}}$ and $B = ln\frac{P_D}{1-P_D}$, then the depth-based and knowledge-aided depth-based detector performance is found in table VI

VI. Summary

In this paper we have introduced a depth-based method for target detection in noisy environments based on a random matrix theoretic pre-detection fusion algorithm to solve for the multistatic response matrix. The performance of the detector was determined for differing levels of noise and compared to two classical monostatic radar system detectors: the single-pulse and envelope detector, respectively. The results demonstrated the benefits of utilizing a distributed sensing network and depth-based algorithms for the detection of a

P_{FA}	Required SNR for Envelope Detector	Required SNR for Depth-Based Detector	Improvement Factor of Depth-Based Detector
6%	5.1 dB	2.8 dB	+2.3 dB
4%	5.6 dB	2.8 dB	+2.6 dB
3%	5.9 dB	3.2 dB	+2.7 dB
10^{-2}	7.2 dB	3.8 dB	+3.4 dB
10^{-3}	9.9 dB	5.8 dB	+4.1 dB
10^{-4}	12.5 dB	9.8 dB	+2.7 dB

TABLE VI: Probability of Detection Comparison for Depth-Based Detector versus Envelope Detector

$k\sigma$	Required SNR for Envelope Detector	Required SNR for Depth-Based Detector	Improvement Factor of Depth-Based Detector
4σ	12.5 dB	2.8 dB	+9.7 dB
5σ	17.9 dB	2.8 dB	+15.1 dB
6σ	23.3 dB	3.2 dB	+20.1 dB
10σ	SNR$\gg$ 26.0 dB	3.8 dB	SNR$\gg$+22.2 dB
32σ	SNR$\gg$26.0 dB	5.8 dB	SNR$\gg$+20.2 dB
100σ	SNR$\gg$26.0 dB	9.8 dB	SNR$\gg$+16.2 dB

TABLE VII: Probability of Detection Comparison for Knowledge-Aided Depth-Based Detector versus Envelope Detector

target obfuscated by a noisy measurement environment. When knowledge of the underlying noise distribution was assumed, the depth-based methods were shown to nominal improve on the classical single-pulse magnitude threshold detector by a factor of up to $+15.1dB$, and a classical envelope detector by a factor of $upto + 20.1dB$.

However, the depth-based detector is nonparametric in formulation, and does not rely on the underlying corruptive noise process to conform to a univariate or bivariate distribution; in fact, the depth-based detector should be more optimal for cases in which the underlying noise process is multivariate and not adequately described by a second-order moment method. Further, while the current depth-based detector is generalized for the underlying corruptive measurement process, it is also generalizable to higher dimensions as well. Currently, the depth-based detector example problem was solved in $\mathbb{R}^d$, where $d = 2$; however, the dimensionality of the problem can be increased to any value of $d = [2, \infty)$, opening up a number of challenge problems for conducting salient signal processing tasks under both *big data* and *high-dimensionality* scenarios.

Current efforts are focused on the extension of this depth-based detector to broader classes of corruptive noise distributions; including those distributions that are not adequately described by second-order moment methods. The authors feel the innovation behind this depth-based approach is that no form of the underlying corruptive noise has to be assumed *a priori*, and in fact, the algorithm is nonparametric in formulation and applicable to any corruptive noise process-both known and unknown.

VII. Conclusion

Depth-based methods lie at the intersection of mathematical statistics and computational geometry, and have been emerged over the past decade as a promising candidate for dealing with high-dimensionality nonparametric multivariate data. While there have been many publications detailing depth-based methods and applications, there are currently no publications that focus on sensing related challenges that could benefit from the incorporation of the depth-based algorithms. In this paper, the authors demonstrated the more salient task of a sensing system-detection-and the detection improvement afforded by the tandem use of a distributed sensing network and a depth-based detection algorithm.

The authors are currently exploring a broad range of sensing modalities that would benefit from this emerging field of mathematical statistics and anticipate further examples of depth-based methodologies to emerge as part of this broader research effort. Follow-on publications will focus on on incorporating statistical ranking and selection into our innovative depth-based detector and formalizing the empirical distribution function utilized for the Neyman-Pearson criterion.

Acknowledgment

The authors gratefully acknowledge the sponsorship of the Air Force Office of Scientific Research, Air Force Material Command, United States Air Force under grant number FA8650-11-RY-09COR.

References

[1] J.L. Hodges, A bivariate test. *Annals of Mathematical Statistics*, vol. 26, pp. 523-527, 1955.

[2] J.W. Tukey, Mathematics and the picturing of data. *Proceedings of the International Congress of Math*, 1975.

[3] R.Y. Liu, J.M. Parelius, K. Singh, Multivariate analysis by data depth: Descriptive statistics, graphic and inference. *The Annals of Statistics*, vol. 27, no. 3, pp. 783-840, 1999.

[4] S. Ghahramani, *Fundamentals of Probability*, 2nd Ed., Prentice Hall, New Jersey, 2000.

[5] G.W. Stimson, *Introduction to Airborne Radar*, Second Ed., SciTech Publishing, Raleigh, NC, 2000.

[6] Y. Zou, and R. Serfling, Structural properties and convergence results for contours of sample statistical depth functions. *The Annals of Statistics*, vol. 28, no. 2, pp. 483-499, 2000.

[7] S. Kingsley, S. Quegan, *Understanding Radar Systems*, SciTech Publishing, Raleigh, NC, 2005.

[8] M.A. Richards, *Fundamentals of Radar Signal Processing*, McGraw-Hill,New York, NY; 2005.

[9] H.Ammari, J.Garnier, and Kut Slna, A Statistical Approach to Target Detection and Localization in the Presence of Noise, *Waves in Random and Complex Media*, 2011.

[10] J. Garnier, Use of Random Matrix Theory for Target Detection, Localization, and Reconstruction, *Contemporary Mathematics*, vol. 548, pp. 151-163, 2011.

[11] T. Tao, Outerliers in the spectrum of IID matrices with bounded rank perturbations, preprint arXiv:1012.4818v4 [math.PR] 7 july 2011.

[12] H.D. Griffiths, "Advances in Bistatic Radar," *IEEE Radar Conference 2012*, Tutorial, Atlanta, GA, 2012.